Biosensors and Bioelectronics 54 (2014) 211–216

Contents lists available at ScienceDirect

Biosensors and Bioelectronics

journal homepage: www.elsevier.com/locate/bios

Voltammetric behavior of uric acid on carbon paste electrode modified with salmon sperm dsDNA and its application as label-free electrochemical sensor

Maryam Mohamadi [a,b,*], Ali Mostafavi [a], Masoud Torkzadeh-Mahani [c]

[a] Department of Chemistry, Shahid Bahonar University of Kerman, Kerman, Iran
[b] Young Research Society, Shahid Bahonar University of Kerman, Kerman, Iran
[c] Department of Biotechnology, Institute of Science, High Technology and Environmental Science, Graduate University of Advance Technology, Kerman, Iran

ARTICLE INFO

Article history:
Received 21 August 2013
Received in revised form
22 October 2013
Accepted 30 October 2013
Available online 13 November 2013

Keywords:
DNA biosensor
Salmon sperm dsDNA
Uric acid
Carbon nano tube paste electrode
Voltammetry

ABSTRACT

A simple and sensitive label-free electrochemical DNA biosensor was proposed for the rapid determination of uric acid (UA) using a carbon nano tube paste electrode (CNTPE) modified with salmon sperm dsDNA. At first, the interaction between UA and the DNA was studied using differential pulse voltammetry (DPV). The addition of the DNA to UA solution resulted in a decrease in the peak current of UA and at the same time, a positive shift in the peak potential indicating an intercalative interaction. Then, the voltammetric response of a DNA-immobilized CNTPE was investigated for the determination of UA. The immobilization of the DNA was carried out using acid-functionalized carbon nanotubes and studied using $Fe(CN)_6^{3-}/Fe(CN)_6^{4-}$ redox indicator. Compared with unmodified CNTPE, the oxidation signal of UA showed a significant increase at the DNA-coated electrode, and shifted to more positive potentials attributed to the pre-concentration of UA at the electrode surface due to interaction with the surface-confined DNA layer. This interaction was used for the fabrication of a simple and sensitive biosensor for determining UA. After the optimization of operational parameters, a linear dependence of the peak current on the UA concentration was observed in the range of 7.0×10^{-7} to 1.1×10^{-4} mol L^{-1}, with the detection and quantification limits of 1.8×10^{-7} and 5.8×10^{-7} mol L^{-1}, respectively. The proposed biosensor was successfully applied to validate its capability for the analysis of UA in human serum and urine samples.

1. Introduction

Biosensors are small devices, which utilize biological reactions for detecting target analytes (Collings and Caruso, 1997). According to an IUPAC definition, a biosensor consists of biorecognition elements specific to the analyte of interest and a physiochemical transducer to relay the resultant signal from this biorecognition event (Chambers et al., 2008).

Electrochemical DNA biosensors comprise a nucleic acid recognition layer, which is immobilized on an electrochemical transducer. The role of the nucleic acid recognition layer is to detect the changes that occurred in the DNA structure during interaction with DNA-binding molecules or to selectively detect a specific sequence of DNA. The signal transducer must determines the change that has occurred in the recognition layer due to the binding molecules or due to the hybridization and converts this to an electronic signal (Gooding, 2002).

DNA interacts reversibly with a broad range of low molecular mass inorganic and organic species, including various carcinogens, antineoplastic drugs, environmental pollutants, etc. (Adams et al., 1986; Wallace et al., 1994). The interaction between small molecules and DNA can be classified into two major categories, intercalation and groove binding. Intercalation involves the insertion of a planar molecule between DNA base pairs, which results in a decrease in the DNA helical twist and lengthening of the DNA (Lerman, 1961). Groove binding includes fitting the molecule into the DNA minor groove causing a slight perturbation of the DNA structure (Chaires, 1998).

The study of interactions between small molecules and DNA is of importance because these interactions are the basis of carcinogenic and therapeutic properties of many carcinogenic species, antitumor and antivirus drugs (Yapasan et al., 2010). In addition, these interactions can be utilized in the construction of DNA biosensors for detection of DNA binders (Lu et al., 2013).

Some substances can be selectively accumulated in electrode surface-confined DNA (Banitaba et al., 2011; Ensafi et al., 2012,

* Corresponding author at: Department of Chemistry, Shahid Bahonar University of Kerman, Kerman, Iran. Tel./fax: +98 341 3222033.
E-mail address: m.mohamadi794@gmail.com (M. Mohamadi).

0956-5663/$ - see front matter © 2013 Elsevier B.V. All rights reserved.
http://dx.doi.org/10.1016/j.bios.2013.10.064

2013; Lu et al., 2004; Mirmoghtadaie et al., 2013). These effects can be utilized in the construction of electrochemical DNA biosensors for the detection of DNA binders. Moreover, electrochemical techniques have been shown to be capable of determination of binding constants, binding modes as well as binding site sizes of the association of DNA with ligands (Aslanoglu, 2006; Gherghi, 2003; Radi et al., 2003; Shah et al., 2008; Wang et al., 2011). The DNA-trapped compounds can either be detected directly (if they are electroactive molecules) or via changes in electrochemical DNA signal. These interactions frequently result in changes of electrochemical responses of the binders due to altered mass transport (Labuda et al., 1999; Rodriguez and Bard, 1992) and/or decreased accessibility of the binder electroactive groups (Carter and Bard, 1987; Rodriguez and Bard, 1990). In addition, alterations of intrinsic DNA electrochemical behavior upon interaction with the ligands can be detected (Fojta et al., 2000).

Uric acid (UA) and other oxypurines are the main final products of purine metabolism in the human body (Huang et al., 2004). The determination of UA in urine is of great importance in medical diagnosis. For example, leucocythemia, heavy hepatitis and gout may cause the increase in the concentration of UA in urine (He et al., 2007).

In the present work, a simple, rapid, low-cost and sensitive electrochemical biosensor was proposed for the determination of uric acid in human serum and urine samples. For this purpose, the interaction of UA with salmon sperm dsDNA in solution was studied with DPV at a carbon nano tube paste electrode. The voltammetric behavior of UA at the electrode surface coated with the dsDNA, was also investigated. Finally, experimental and operational parameters were optimized for the determination of UA at the dsDNA-coated carbon nano tube paste electrode. The capability of the biosensor was then validated by the determination of UA in human serum and urine samples.

2. Experimental

2.1. Apparatus

All voltammetric experiments were performed with an Autolab PGSTAT 101 electrochemical system from Metrohm (Switzerland) interfaced with a personal computer for data acquisition and potential control. A three-electrode system was used consisted of a platinum wire as the auxiliary electrode, Ag/AgCl/KCl (saturated) as the reference electrode and a carbon nano tube paste electrode (CNTPE) as the working electrode. All pH measurements were carried out using a Metrohm 827 pH meter (Herisau, Switzerland) supplied with a combination glass-reference electrode.

2.2. Reagents and materials

A 0.010 mol L^{-1} stock solution of the uric acid obtained from Alpha Aesar (Karlsruhe, Germany) was prepared by dissolving the appropriate amount of the solid in a small volume of 0.1 mol L^{-1} NaOH solution and diluting it to the desired volume. Salmon sperm double stranded DNA (dsDNA) was purchased from Sigma (St. Louis, USA). A 1.0 mg mL^{-1} stock solution of the DNA was prepared in Tris–HCl (TE) buffer (pH 7.4) and kept frozen. Multi-walled carbon nanotubes (MWCNT) with 95% purity, length of 1–10 μm and the number of walls varying from 3 to 15 were purchased from Plasma Chem. GmbH (Germany). Pure graphite powder, sodium dihydrogen phosphate, sodium acetate, acetic acid, phosphoric acid, hydrochloric acid and methanol were purchased from Merck (Darmstadt, Germany).

2.3. Sample preparation

Human serum and urine samples were obtained and stored in a refrigerator at 4 °C until analyzed. The samples were prepared according to the literature with minor modifications (Wang et al., 2011). Aliquots of the urine sample (1.0 mL) were spiked with given amounts of UA and then treated with 0.1 mL of methanol to precipitate the urine proteins. After stirring the sample for approximately 30 s, the precipitated proteins were separated by centrifugation at 3000 rpm for 30 min. The clear, protein-free supernatant layer was filtered through the 0.45-μm Millipore filter and diluted to 100 mL with 0.50 mol L^{-1} acetate buffer (pH 5.20).

One milliliter of the serum sample was transferred into each of the centrifuge tubes containing different known amounts of UA and then mixed well with 10 mL of methanol to precipitate the blood proteins. After centrifugation at 3000 rpm for 30 min and separation of precipitated proteins, the clear supernatant layer was filtered through the 0.45-μm Millipore filter and then diluted to 50 mL with 0.50 mol L^{-1} acetate buffer (pH 5.20).

2.4. Functionalization of MWCNTs

Prior to use, MWCNTs were pretreated as described in the literature (Shamspur and Mostafavi, 2009) but with minor modification. One gram of the raw MWCNTs was thermally treated using a furnace at 400 °C for 40 min to remove amorphous carbon and then soaked in 10 mL of HNO_3 6 mol L^{-1} for 20 h at room temperature while being stirred. The solid product was collected on a 0.45-μm Millipore filter and washed several times with distilled water until the pH was neutral. The obtained functionalized MWCNTs were then dried in an oven at 80 °C for 24 h.

2.5. Preparation of carbon nano tube paste electrode

A carbon nano tube paste electrode (designated as CNTPE) was prepared by mixing graphite powder and the functionalized MWCNTs with 90/10 (w/w) ratio using a mortar and pestle. Paraffin oil was added to the above mixture and mixed until a uniformly wetted paste was obtained. This paste was then packed into the end of a glass tube (3.4 mm inner diameter). Electrical contact was established via a copper wire connected to the paste. The electrode surface was gently smoothed by rubbing it on a piece of filter paper just prior to use. When necessary, a new surface was obtained by pushing a bit of the paste out of the tube. Bare electrode was prepared in the same way without adding of MWCNTs (designated as bare CPE).

2.6. Immobilization of the dsDNA on the CNTPE surface

The dsDNA was immobilized on the CNTPE as described in the literature (Kara et al., 2002) by applying a potential at 0.50 V in 10 mL of 0.50 mol L^{-1} acetate buffer solution (pH 4.80) containing 10 mg L^{-1} of the dsDNA while stirring for 400 s. The electrode was then rinsed with acetate buffer solution. The obtained electrode will henceforth be called dsDNA-coated CNTPE.

2.7. Cyclic voltammetry of $K_3[Fe(CN)_6]$

The cyclic voltammogram of 2.0 mmol L^{-1} $K_3Fe(CN)_6$ in 0.01 mol L^{-1} PBS and 0.50 mol L^{-1} KNO_3 was recorded from −200 to 500 mV using a scan rate of 100 mV s^{-1}.

2.8. Adsorptive stripping differential pulse voltammetry at dsDNA-coated CNTPE

The dsDNA-coated CNTPE was dipped into 10 mL acetate buffer (0.50 mol L^{-1}, pH 5.20) containing different concentrations of UA, and the solution was stirred at an open circuit system for different times (accumulation step). The electrode was then rinsed with distilled water and placed in 10 mL of 0.30 mol L^{-1} phosphate buffer solution (pH 3.00). Voltammograms were recorded by scanning the potential towards the positive direction from +300 to +700 mV using the differential pulse mode which employed a step potential of 10 mV and modulation amplitude of 50 mV (stripping step).

3. Results and discussions

3.1. Cyclic voltammetry study on the immobilization of DNA onto CNTPE

Cyclic voltammetry (CV) of $Fe(CN)_6^{3-}/Fe(CN)_6^{4-}$ redox couple, as the indicator, was used for the study of DNA immobilization on the CNTPE surface. The function of this indicator is based on the electrostatic repulsion of the redox couple and the negatively charged DNA phosphate backbone (Ovádeková et al., 2006). Fig. 1 shows the typical cyclic voltammograms of the immobilization process. At the bare CPE, the voltammogram of $K_3[Fe(CN)_6]$ was characterized by a pair of well-defined peaks with a cathodic peak potential (E_{pc}) of 117 mV and an anodic peak potential (E_{pa}) of 339 mV and the peak-to-peak potential separation (ΔE_p) of 222 mV (curve a in Fig. 1). The currents of both peaks showed an increase using CNTPE. In addition, the redox reversibility of Fe $(CN)_6^{3-}$ was improved in the presence of CNTs while ΔE_p decreased to 154 mV (curve b in Fig. 1).

After the immobilization of dsDNA on the CNTPE surface, an increase in the ΔE_p to 396 mV was observed indicating the decrease of the electrochemical reversibility of the $Fe(CN)_6^{3-}/Fe$ $(CN)_6^{4-}$ redox couple at the DNA-coated electrode (curve c in Fig. 1). At the same time, both the anodic and cathodic peak currents decreased. This decrease may be explained as follows: after the immobilization of dsDNA on the CNTPE, the negatively charged phosphate groups on dsDNA resist the access of the Fe $(CN)_6^{3-}/Fe(CN)_6^{4-}$ redox couple to the electrode surface due to electrostatic repulsion (Maruyama et al., 2001). Consequently, the difference between the CV profiles for these electrodes enables detection of the immobilization of the dsDNA on the surface of the electrodes.

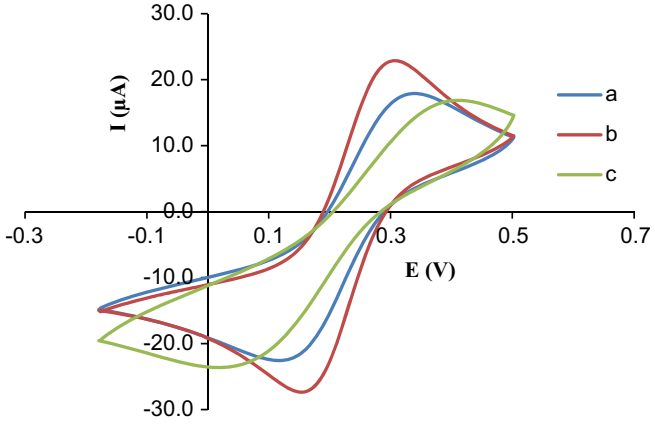

Fig. 1. Cyclic voltammograms of (a) bare CPE, (b) CNTPE and (c) dsDNA-coated CNTPE in 0.01 mol L^{-1} PBS containing 2.0 mmol L^{-1} $K_3Fe(CN)_6$ and 0.50 mol L^{-1} KNO_3. Conditions: potential range −0.20 to 0.50 V at a scan rate of 100 mV s^{-1}.

3.2. Interaction between UA and the dsDNA in solution

DP voltammogramms of UA in phosphate buffer (0.50 mol L^{-1}, pH 5.20) recorded in the absence and presence of the dsDNA, were shown in Fig. 2A. As can be seen, after adding the dsDNA and incubating for 5 min the oxidation signal of UA doubled with a positive shift in the peak potential (55 mV). Such results may be attributed to one of the following two factors: (i) the non-conducting DNA could block the electron transfer between UA and electrode surface or (ii) the DNA–UA complex formed was electrochemically inactive (Wang et al., 2011). If the electron transfer was blocked, then the current should decrease (relative to that of the clean electrode) but no peak shift would be expected.

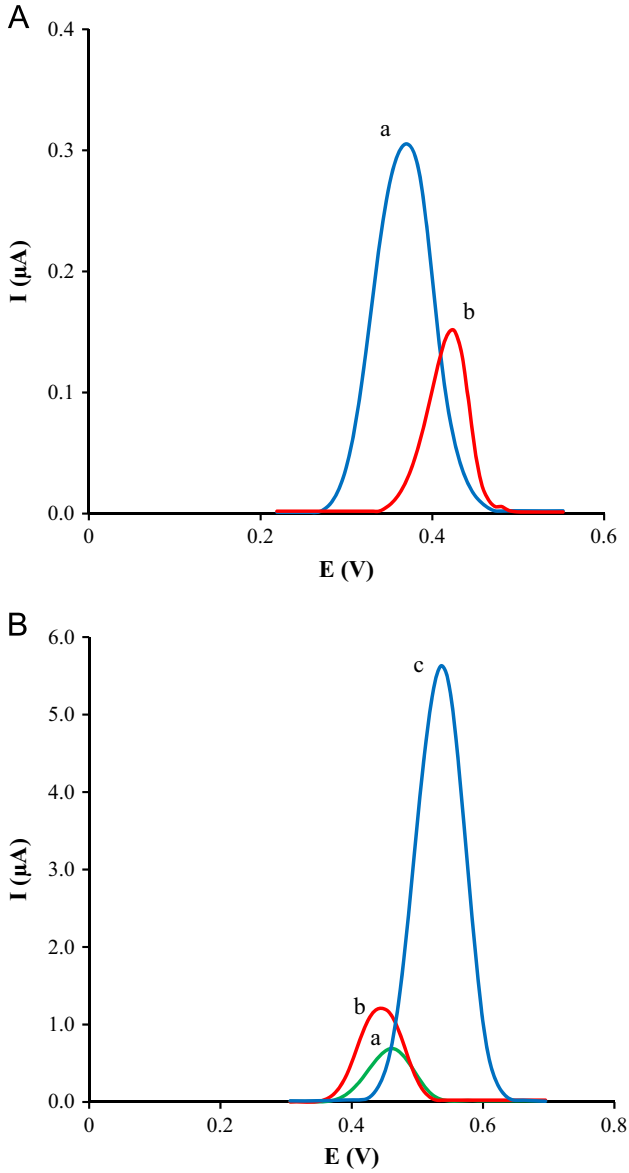

Fig. 2. (A) DP voltammograms of 6.0×10^{-5} mol L^{-1} UA at CNTPE in 0.5 mol L^{-1} acetate buffer of pH 5.20 in the absence of the dsDNA (a) and in the presence of 20 μg mL^{-1} of the dsDNA (b). Incubation time, 5 min. (B) DP voltammograms obtained after accumulation of UA at bare CPE (a), CNTPE and dsDNA-coated CNTPE. Conditions: UA concentration 5.0×10^{-5} mol L^{-1}, accumulation medium 0.50 mol L^{-1} acetate buffer pH 5.20, accumulation time 5 min, stripping medium 0.30 mol L^{-1} phosphate buffer pH 3.00.

In the presence of DNA, the current is mainly due to unbound species, since the diffusion rate of the DNA-bound species is small (Welch and Thorp, 1996). So, this observed decrease in the anodic current of UA is attributed to the decrease in the unbound UA concentration due to the formation of the UA–DNA complex which is a consequence of DNA addition.

Furthermore, the peak potential shifted to more positive value after interaction with the dsDNA. As mentioned in the literature (Lu et al., 2004), a negative shift in peak potential is a characteristic of an electrostatic mode interaction between DNA and desired specie while a positive shift indicates an interaction of intercalative mode. Accordingly, the positive shift in the peak potential of UA is attributed to a characteristic behavior of the intercalation of UA into the DNA double helix.

According to these observations, it seems that the decrease of peak current of UA after addition of the dsDNA is caused by the intercalation of UA into the bulky, slowly diffusing DNA, which results in a considerable decrease in the apparent diffusion coefficient.

3.3. Electrochemical behavior of UA at the surface of dsDNA-coated CNTPE

Fig. 2B shows DP voltammograms obtained after accumulation of UA at bare CPE (curve a), CNTPE (curve b) and dsDNA-coated CNTPE (curve c) from a stirring 5.0×10^{-5} mol L^{-1} UA in 0.50 mol L^{-1} acetate buffer (pH 5.20) for 5 min at open circuit condition, followed by washing the electrode with distilled water and transferring it into blank 0.30 mol L^{-1} phosphate buffer (pH 3.00) as the supporting electrolyte.

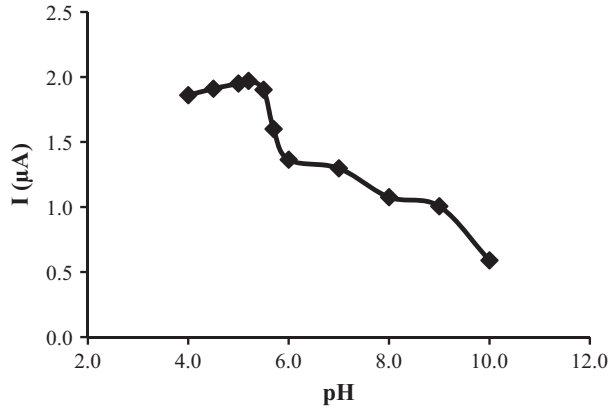

Fig. 3. Effect of accumulation pH on the DP voltammograms of UA accumulated at dsDNA-coated CNTPE. Conditions: UA concentration 2.0×10^{-5} mol L^{-1}, other conditions were the same as given in Fig. 2B, except acetate buffer pH.

As one can see from Fig. 2B, E_{pa} shows a positive shift at the dsDNA-coated electrode relative to bare CPE and CNTPE. In addition, the dsDNA-coated electrode exhibits the largest anodic signal, reflecting the interaction of UA with the DNA layer immobilized on the electrode surface. In other words, this enhanced sensitivity is a result of the pre-concentration due to the adsorption of UA on the surface of the electrode through a strong interaction.

Cyclic voltammetry of 5.0×10^{-6} mol L^{-1} UA was carried out at different scan rates (ν) (Fig. S1A). In the forward scan, a single anodic peak was observed, which corresponds to the oxidation of UA. In the reverse scan, no cathodic peak is observed, which indicates that the process is irreversible.

A linear plot of I_{pa} versus ν (Fig. S1B) was obtained in the range of 10–150 mV s^{-1} at the dsDNA-coated CNTPE, indicating the oxidation of UA molecules associated with the immobilized DNA. In addition, E_{pa} shifted positively with increasing scan rate, as expected for an irreversible electrode process (Radi et al., 2003).

3.4. Optimization of experimental and operational parameters

In order to use the dsDNA-coated CNTPE for UA determination in real samples, the main experimental parameters affecting the biosensor response were optimized.

3.4.1. Immobilization time

The effect of the dsDNA immobilization time on I_{pa} of the accumulated UA was investigated using DPV. It was observed that the amount of adsorbed DNA rose with increasing the immobilization time and started to saturate at approximately 400 s. Accordingly, the immobilization time of 400 s was used in further studies.

3.4.2. Accumulation pH

Influence of pH on the interaction between UA and the dsDNA immobilized on the electrode surface and subsequent accumulation of UA on the electrode surface was studied in the range of 4.00–10.00. According to the results shown in Fig. 3, when the pH increases to more than 5.50, the anodic signal of UA starts to decrease while the optimum pH value was around 5.20. At higher pHs, UA forms the negatively charged urate or hydrogen urate ions. Electrostatic repulsion between the UA ions and negatively charged DNA reduces the UA concentration near the electrode surface which results in the decrease of oxidation signal of UA. In subsequent experiments, accumulation pH was adjusted to the optimal value 5.20.

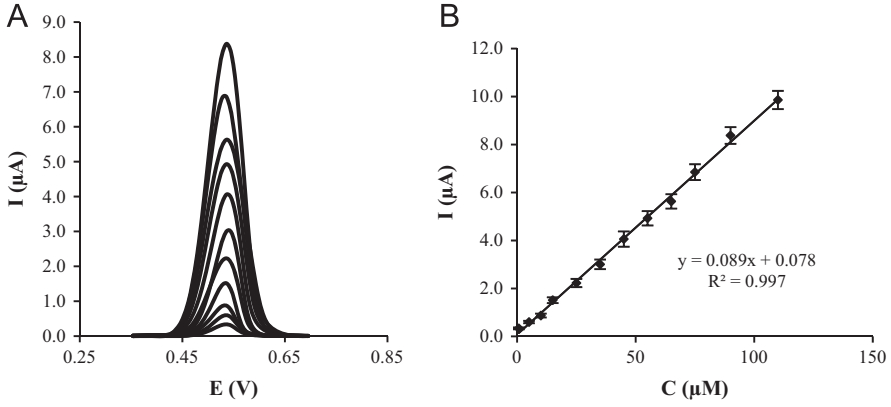

Fig. 4. Differential pulse voltammograms obtained at dsDNA-coated CNTPE for UA at different concentrations (a–k) 7.0×10^{-7}, 5.0×10^{-6}, 1.0×10^{-5}, 1.5×10^{-5}, 2.5×10^{-5}, 3.5×10^{-5}, 4.5×10^{-5}, 5.5×10^{-5}, 6.5×10^{-5}, 7.5×10^{-5}, 9.0×10^{-5} and 1.10×10^{-3} mol L^{-1}, respectively. Corresponding RSDs of I: 11.8–3.8%. Other conditions were the same as given in Fig. 2B.

3.4.3. Effect of accumulation time

The interaction of UA with the dsDNA is dependent on the accumulation time. The dependence of the I_{pa} of UA on the time of accumulation was studied in acetate buffer pH 5.20 at a dsDNA-coated CNTPE. For the first 5 min, an increase was observed while at longer accumulation times, a leveling-off (Fig. S2). So, accumulation was performed for 5 min in all experiments.

3.4.4. Stripping pH

Since proton takes part in the oxidation of UA, the pH value of solution will greatly influence the I_{pa} (Luo et al., 2005). Accordingly, the effect of stripping pH on the response of the biosensor was evaluated in phosphate buffer 0.30 mol L^{-1} and pH values ranging from 2.00 to 6.00. The results showed a maximum of I_{pa} when the buffer solution pH was 3.00 (Fig. S3). Therefore, in subsequent experiments the stripping was carried out in 0.30 mol L^{-1} phosphate buffer with pH 3.00.

3.4.5. Stripping medium concentration

The effect of the concentration of phosphate buffer (pH 3.00) used as supporting electrolyte in stripping medium, was investigated for the highest oxidation signal of UA. The results (Fig. S4) showed that the I_{pa} increased with increase of the buffer concentration in the range of 0.10–0.30 mol L^{-1} and then remained constant when the amount was continuously increased up to 0.40 mol L^{-1}. Hence, a phosphate buffer 0.30 mol L^{-1} was selected as the stripping medium for further studies.

3.5. Analytical performance

The proposed DNA biosensor was validated with respect to linearity, precision, limit of detection (LOD) and limit of quantification (LOQ). Fig. 4 shows the DPV response of dsDNA-coated CNTPE for different UA concentrations (A), and a calibration curve for UA detection with the proposed biosensor under the optimal experimental conditions (B). The calibration graph exhibits a linear relationship between the peak current at dsDNA-coated CNTPE and the UA concentration over the range of 7.0×10^{-7}–1.1×10^{-4} mol L^{-1} with a slope of 0.089 μA mol L^{-1}, intercept of 0.078 μA and correlation coefficient of 0.997.

Reproducibility was assessed by five replicate measurements (after accumulation on dsDNA-coated CNTPE) at 5.0×10^{-6} and 5.0×10^{-5} mol L^{-1} of UA; the corresponding RSDs were calculated to be 9.6% and 5.7%, respectively. Theoretical LOD and LOQ (calculated as three and ten times of the standard deviation of the blank, respectively) were found to be 1.8×10^{-7} and 5.8×10^{-7} mol L^{-1}, respectively.

Table 1
Analytical results of spiked human plasma and urine.

Sample	Added (μM)	Found[a] (μM)	Recovery (%)	Total value[b] (mM)
Urine	–	34.2 ± 2.1	–	3.42
	20.0	53.7 ± 3.2	97.5	–
	50.0	85.6 ± 3.4	102.8	–
Serum	–	6.2 ± 0.6	–	0.31
	10.0	16.4 ± 1.3	102.0	–
	50.0	55.4 ± 3.0	98.4	–

[a] Mean ± standard deviation (n=3).
[b] Total value was obtained by multiplying the detected value by the appropriate dilution factor (100 for urine and 50 for serum samples).

3.6. Inferences of coexisting compounds

The effects of some possible interfering compounds such as urea, ascorbic acid, folic acid and glucose on the UA determination were investigated. According to the results reported in Table S1, there is no significant interference on the I_{pa} of UA.

3.7. Comparison with other sensors

dsDNA-coated CNTPE presented here was compared with some other electrochemical sensors (Ping et al., 2012; Zheng et al., 2013; Hudari et al., 2013; Alipour et al., 2012; Wang et al., 2012; Cui et al., 2012; Sheng et al., 2012; Li et al., 2012) currently reported for the determination of UA. Table 2 shows the results of the comparison. As one can see, the proposed biosensor shows a reasonably low LOD (1.8×10^{-7} mol L^{-1}) and a calibration range comparable to or better than, the other methods.

3.8. Application of the dsDNA-coated CNTPE

Human serum and urine samples were selected as real samples for analysis by the proposed biosensor using the standard addition method. For the determination of UA in each sample, the dsDNA-coated CNTPE was immersed into 10 mL of the prepared sample solution while stirring at an open circuit condition for 5 min (accumulation step). After medium exchange for blank phosphate buffer solution (0.30 mol L^{-1}, pH 3.00), DP voltammogram was recorded. Pulse amplitude of 50 mV, pulse width of 50 ms, and step potential of 10 mV, between +300 and +700 mV (stripping step) were applied. The obtained results were reported in Table 1. As can be seen, the spiked recoveries are satisfactory and confirm that the proposed biosensor is applicable for determining UA in biological samples.

4. Conclusions

An electrochemical biosensor was proposed for the determination of uric acid based on its interaction with salmon sperm dsDNA. The interaction between UA and the dsDNA in solution was probed by DPV at CNTPE. The mode of the interaction was

Table 2
Comparison of the presented method with some electrochemical sensors currently reported for the determination of uric acid.

Electrode	Linear range (μmol L^{-1})	LOD (μmol L^{-1})	Ref.
GCE[a] modified with 4-aminobutyric acid	1.0–80.0	0.5	Zheng et al. (2013)
High-performance screen-printed graphene electrode	0.8–2500	0.20	Ping et al. (2012)
MWCNT paste electrode	5.0–92.6	0.25	Hudari et al. (2013)
Pretreated pencil graphite electrode	1–160	0.19	Alipour et al. (2012)
poly (acridine orange)/graphene modified electrode	0.1–1000	0.02	Wang et al. (2012)
Helical carbon nanotubes modified electrode	6.7–65	1.5	Cui et al. (2012)
Nitrogen doped graphene	0.1–20	0.045	Sheng et al. (2012)
GCE modified with graphene and poly(acridine red)	0.8–150	0.3	Li et al. (2012)
dsDNA-coated CNTPE	0.7–110	0.18	Present work

[a] Glassy carbon electrode.

found to be intercalation. We also investigated the oxidation of UA at the CNTPE coated with the dsDNA. Considerable increase in I_{pa} along with a positive potential shift at the modified electrode relative to unmodified CNTPE, represented the pre-concentration of UA at the electrode surface due to the interaction with the dsDNA. After optimizing the main experimental parameters, the performance of this fabricated DNA-coated CNTPE was evaluated from the analytical point of view. As real samples, human serum and urine samples were successfully analyzed for UA determination with the proposed biosensor. Finally, it is believed that the label-free DNA-coated CNTPE possesses the advantages of rapidity, sensitivity, simplicity of operation, low cost and is applicable to biological samples.

Acknowledgment

This work was supported by grants from the Research Council of Shahid Bahonar University of Kerman.

Appendix A. Supplementary material

Supplementary data associated with this article can be found in the online version at http://dx.doi.org/10.1016/j.bios.2013.10.064.

References

Adams, R.L.P., Knowler, J.T., Leader, D.P., 1986. The Biochemistry of the Nucleic Acids. Chapman and Hall, New York.
Alipour, E., Majidi, M.R., Saadatirad, A., Golabi, S.M., 2012. Anal. Methods 4, 2288–2295.
Aslanoglu, M., 2006. Anal. Sci. 22 (3), 439–443.
Banitaba, M.H., Davarani, S.S., Mehdinia, A., 2011. Anal. Biochem. 411 (2), 218–222.
Carter, M.T., Bard, A.J., 1987. J. Am. Chem. Soc. 109 (24), 7528–7530.
Chaires, J.B., 1998. Curr. Opin. Struct. Biol. 8 (3), 314–320.
Chambers, J.P., Arulanandam, B.P., Matta, L.L., Weis, A., Valdes, J.J., 2008. Curr. Issues Mol. Biol. 10 (1), 1–12.
Collings, A.F., Caruso, F., 1997. Rep. Prog. Phys. 60 (11), 1397–1445.
Cuia, R., Wanga, X., Zhangb, G., Wang, C., 2012. Sens. Actuators B: Chem. 161, 1139–1143.
Ensafi, A.A., Heydari-Bafrooei, E., Amini, M., 2012. Biosens. Bioelectron. 31 (1), 376–381.
Ensafi, A.A., Heydari-Bafrooei, E., Rezaei, B., 2013. Biosens. Bioelectron. 41, 627–633.
Fojta, M., Havran, L., Fulnečková, J., Kubičárová, T., 2000. Electroanalysis 12 (12), 926–934.
Gherghi, I., 2003. Talanta 61 (2), 103–112.
Gooding, J.J., 2002. Electroanalysis 14 (17), 1149–1156.
He, J.-B., Jin, G.-P., Chen, Q.-Z., Wang, Y., 2007. Anal. Chim. Acta 585 (2), 337–343.
Huang, S.-H., Shih, Y.-C., Wu, C.-Y., Yuan, C.-J., Yang, Y.-S., Li, Y.-K., Wu, T.-K., 2004. Biosens. Bioelectron. 19 (12), 1627–1633.
Hudaria, F.F., Duartea, E.H., Pereirab, A.C., Dall'Antoniaa, L.H., Kubotac, L.T., Tarley, C.R.T., 2013. J. Electroanal. Chem. 696, 52–58.
Kara, P., Kerman, K., Ozkan, D., Meric, B., Erdem, A., Nielsen, P.E., Ozsoz, M., 2002. Electroanalysis 14 (24), 1685–1690.
Labuda, J., Bučková, M., Vaníčková, M., Mattusch, J., Wennrich, R., 1999. Electroanalysis 11 (2), 101–107.
Lerman, L., 1961. J. Mol. Biol. 3 (1). (18-IN14).
Li, Y., Ran, G., Yi, W.J., Luo, H.Q., Li, N.B., 2012. Microchim. Acta 178, 115–121.
Lu, X., Zhang, M., Kang, J., Wang, X., Zhuo, L., Liu, H., 2004. J. Inorg. Biochem. 98 (4), 582–588.
Lu, Y., Li, X., Wang, G., Tang, W., 2013. Biosens. Bioelectron. 39 (1), 231–235.
Luo, J.-W., Zhang, M., Pang, D.-W., 2005. Sens.Actuators B: Chem. 106 (1), 358–362.
Maruyama, K., Motonaka, J., Mishima, Y., Matsuzaki, Y., Nakabayashi, I., Nakabayashi, Y., 2001. Sens. Actuators B: Chem. 76 (1), 215–219.
Mirmoghtadaie, L., Ensafi, A.A., Kadivar, M., Norouzi, P., 2013. Mater. Sci. Eng. C: Mater. Biol. Appl. 33 (3), 1753–1758.
Ovádeková, R., Jantová, S., Letašiová, S., Štepánek, I., Labuda, J., 2006. Anal. Bioanal. Chem. 386 (7–8), 2055–2062.
Ping, J., Wu, J., Wang, Y., Ying, Y., 2012. Biosens. Bioelectron. 34, 70–76.
Radi, A., El Ries, M.A., Kandil, S., 2003. Anal. Chim. Acta 495 (1–2), 61–67.
Rodriguez, M., Bard, A.J., 1990. Anal. Chem. 62 (24), 2658–2662.
Rodriguez, M., Bard, A.J., 1992. Inorg. Chem. 31 (7), 1129–1135.
Shah, A., Qureshi, R., Janjua, N.K., Haque, S., Ahmad, S., 2008. Anal. Sci. 24 (11), 1437–1441.
Sheng, Z.-H., Zheng, X.-Q., Xu, J.- N., Bao, W.-J., Wang, F.-B., Xia, X.-H., 2012. Biosens. Bioelectron. 34, 125–131.
Shamspur, T., Mostafavi, A., 2009. J. Hazard. Mater. 168 (2), 1548–1553.
Wallace, S.S., van Houten, B., Kow, Y.W., 1994. DNA Damage: Effects on DNA Structure and Protein Recognition. New York Academy of Sciences.
Wang, Y., Ni, Y., Kokot, S., 2011. Anal. Biochem. 419 (2), 76–80.
Wang, Z., Xia, J., Zhu, L., Zhang, F., Guo, X., Li, Y., Xia, Y., 2012. Sens. Actuators B: Chem. 161, 131–136.
Welch, T.W., Thorp, H.H., 1996. J. Phys. Chem. 100 (32), 13829–13836.
Yapasan, E., Caliskan, A., Karadeniz, H., Erdem, A., 2010. Mater. Sci. Eng. B: Solid State Mater. Adv. Technol. 169 (1–3), 169–173.
Zheng, X., Zhou, X., Ji, X., Lin, R., Lin, W., 2013. Sens. Actuators B: Chem. 178, 359–365.